

MIT Open Access Articles

*Fuel retention measurements in Alcator C-Mod using
accelerator-based in situ materials surveillance*

The MIT Faculty has made this article openly available. **Please share**
how this access benefits you. Your story matters.

Citation: Hartwig, Zachary S. et al. "Fuel Retention Measurements in Alcator C-Mod Using Accelerator-Based in Situ Materials Surveillance." *Journal of Nuclear Materials* 463 (August 2015): 73–77 © 2014 Elsevier B.V.

As Published: <http://dx.doi.org/10.1016/j.jnucmat.2014.09.056>

Publisher: Elsevier

Persistent URL: <http://hdl.handle.net/1721.1/111187>

Version: Author's final manuscript: final author's manuscript post peer review, without publisher's formatting or copy editing

Terms of use: Creative Commons Attribution-NonCommercial-NoDerivs License



Fuel retention measurements in Alcator C-Mod using Accelerator-based In-situ Materials Surveillance

Zachary S. Hartwig^{a,*}, Harold S. Barnard^a, Brandon N. Sorbom^a,
Richard C. Lanza^b, Bruce Lipschultz^c, Peter W. Stahle^b, Dennis G. Whyte^a

^a *Plasma Science and Fusion Center, MIT, Cambridge MA 02139, U.S.A.*

^b *Department of Nuclear Science and Engineering, MIT, Cambridge MA 02139, U.S.A.*

^c *York Plasma Institute, University of York, York, YO10 5DQ, U.K.*

Abstract

This paper presents the first *in-situ* time- and space-resolved measurements of deuterium (D) fuel retention in plasma-facing component (PFC) surfaces using Accelerator-based In-situ Materials Surveillance (AIMS) on the Alcator C-Mod tokamak. AIMS is a novel *in-situ* materials diagnostic technique based on the spectroscopic analysis of nuclear reaction products induced in PFC surfaces using an \sim MeV beam of deuterons from a compact linear accelerator in between plasma shots. AIMS measurements of D retention on inner wall PFCs were acquired during diverted and limited plasma operations and during wall conditioning experiments. Intershot measurements demonstrate the local erosion and codeposition of boron films on PFC surfaces **with a constant D/B ratio**. This is consistent with previous results suggesting that D codeposition with boron is insufficient to account for the net retention observed in Alcator C-Mod. Changes in deuterium concentration during boronization, electron cyclotron and glow cleanings were also measured.

PACS: 52.40.Hf, 52.55.Fa, 52.55.Rk

PSI-20 keywords: Retention, Erosion & deposition, Surface analysis, Divertor diagnostic, Alcator C-Mod.

**Corresponding author address:* 77 Massachusetts Ave, NW17-115, Cambridge MA 02139, U.S.A.

**Corresponding author email:* hartwig@psfc.mit.edu

Presenting author: Zachary S. Hartwig

Presenting author email: hartwig@psfc.mit.edu

1 Introduction

The retention of hydrogenic fusion fuel in plasma-facing component (PFC) surfaces is one of the most challenging aspects of plasma-material interaction (PMI). Fuel saturation of material surfaces and thermal desorption result in fuel recycling between the wall and plasma. The result is a loss of plasma fueling efficiency, plasma density control, and high levels of neutral hydrogen density, ultimately **affecting** the particle and energy confinement of the core plasma. The bulk retention of tritium in PFCs is a serious nuclear safety concern and a facility operations issue, since radioactive decay and diffusive losses of retained tritium can lead to an unacceptably low tritium breeding ratios [1].

Retention has also historically been difficult to comprehensively diagnose *in-situ*. Measurement techniques have tended to extremes in terms of spatial information, with global (*i.e.* zero spatial resolution) measurements such as static gas balance or thermal desorption spectroscopy at one end and high spatial resolution measurements at only one or two remote locations such as laser desorption spectroscopy at the other end [2]. Although promising advances have been made with laser-based measurement techniques, such as laser-induced breakdown spectroscopy (LIBS) [3], such approaches have been limited to small PFC surface areas and are intrinsically destructive to surface layers. In contrast, a new diagnostic technique recently developed on the Alcator C-Mod tokamak, known as Accelerator-based In-situ Materials Surveillance (AIMS), is capable of making fuel retention measurements - as well as low-Z erosion/redeposition measurements - over large fractions of PFC surfaces with spatial resolution on the order of 1 cm and a time resolution on a plasma shot-to-shot timescale [4, 5, 6, 7]. A graphical overview of the AIMS technique is presented in Figure 1 for reference.

2 The role of boron in fuel retention on Alcator C-Mod

An exhaustive study of hydrogenic fuel retention in Alcator C-Mod has been published, demonstrating that 20-50% of fueled deuterium gas was consistently retained per quiescent discharge with no saturation evident after ~ 25 s of plasma [8]. Unlike hydrogenic retention in tokamaks with carbon (C) PFCs, where the infinite source of eroded C is principally responsible for retention through codeposition, the study showed that the deuterium (D) retention in Alcator C-Mod must occur in the bulk of the molybdenum (Mo) PFCs and not in the thick amorphous thin film layers of boron (B) that accumulate in the machine. Several mechanisms, including energetic fuel ion implantation, diffusion, and retention in created or expanded atomic traps within the bulk Mo lattice, have been proposed to account for D retention in Alcator C-Mod.

Boronization (BZN) is a process by which a low-temperature plasma discharge in diborane (B_2D_6) and helium-4 gas is used to deposit ~ 150 nm thick B films on PFC surfaces via RF-induced breakup of the gas molecules; typically, BZNs on Alcator C-Mod use a 10% diborane / 90% helium-4 mixture. *Ex-situ* analysis has shown that the B layers created by BZN are saturated immediately after deposition with D/B atomic ratios of ~ 0.4 ; rapid D outgassing in the approximately 40 following plasma discharges leads to D/B atomic ratios of ~ 0.1 in Alcator C-Mod, which are measured via static gas balance and post-mortem analysis [8]. During lower single null diverted plasma - the primary configuration in Alcator C-Mod - the B layer is eroded by the plasma from the outer divertor near the separatrix strikepoint and transported to the inner wall and divertor, resulting in 5-10 μm layers of B after several plasma campaigns [9, 10]. This behavior is consistent with material migration observations in other tokamaks, such as JET and ASDEX-Upgrade [11].

The strong poloidal correlation found in post-mortem analysis between D and B concentration suggests that - after the post-BZN D outgassing discussed above has occurred - the plasma erodes and locally codeposits B layers with a constant D/B ratio of ~ 0.1 . This has important consequences for understanding D retention in Alcator C-Mod. In order for D

retention in B films to approach the experimentally observed level, the global B layer would somehow have to be completely depleted ($D/B \sim 0$) and then refilled with D to saturation ($D/B \sim 0.4$) during plasma operations; however, *if the D/B atomic ratio during plasma operation remains constant after post-BZN outgassing then D codeposition with B cannot explain the net retention of D experimentally observed in Alcator C-Mod.* In other words, after post-BZN D outgassing, the plasma is merely shifting around a constant amount of D within the global B film layer. While campaign-integrated post-mortem PFC analysis suggests this is true, AIMS provides for the first time an opportunity to observe the relative changes of D and B in codeposited layers in response to plasma operation on a shot-to-shot timescale.

3 Overview of AIMS experiments during the FY12 campaign

The first substantive AIMS measurements were acquired at the end of the FY12 plasma campaign and encompassed both plasma shots and wall conditioning experiments. A timeline depicting the sequence of tokamak operations and PFC surface measurements is shown in Figure 2.

3.1 Plasma operation

Two very different plasma configurations were chosen in order to maximize the contrast in the configuration-dependent PMI at the inner wall PFCs that are presently accessible for AIMS measurements, as shown in Figure 3. Lower single null (LSN) diverted plasmas were used since previous experience on Alcator C-Mod has shown that eroded material from the outer divertor migrates in the boundary plasma of Alcator C-Mod and strongly net deposits on the inner wall and inner divertor in this configuration [8, 9]. Inner wall limited (IWL) plasma, were chosen since the high-power plasma exhaust in the scrape off layer is directly

incident upon the inner wall PFCs accessible to AIMS, leading to conditions on the inner wall PFCs that result in strong net erosion.

As shown in the timeline of Figure 2, first a series of eighteen, nearly identical lower single null (LSN) diverted shots were taken with flat top parameters of $n_{\bar{e}} \approx 1.3 \times 10^{20} \text{ m}^{-3}$, $T_e \approx 4 \text{ keV}$, $I_p \approx 1.0 \text{ MA}$, and $P_{RF} \approx 3 \text{ MW}$ of ICRF heating. Next, a series of five IWL discharges were run with one of them terminating in a radiative disruption. The IWL flat top parameter were $n_{\bar{e}} \approx 1.3 \times 10^{20} \text{ m}^{-3}$, $T_e \approx 3 \text{ keV}$, $I_p \approx 0.8 \text{ MA}$, and $P_{RF} \approx 2 \text{ MW}$ of ICRF heating. The plasma parameters for LSN and IWL were kept as constant possible such that total erosion/deposition divided by the total plasma time is representative of net thickness change rates. The single IWL disruption terminated early in the discharge with a very small core electron temperature ($\approx 0.75 \text{ keV}$) and stored plasma energy ($\approx 30 \text{ kJ}$), below the experimental threshold for disruption-induced D recovery from a mixed Mo-B surface [12]. Such a small disruption is unlikely to recover significant D even from a pure B layer despite potentially higher temperature rise relative to the mixed Mo-B surface.

3.2 Wall conditioning

Following the conclusion of the plasma campaign, a series of AIMS-specific wall conditioning operations were performed in order to measure response of the inner wall PFC surfaces.

As shown on the timeline in Figure 2, three different wall conditioning procedures were carried out: BZN, electron cyclotron discharge cleaning (ECDC), and glow discharge cleaning (GDC). The 120 minute BZN was performed with a gas mixture of 10% diborane (B_2D_6) / 90% helium-4 at an average vessel pressure of $2.7 \times 10^{-3} \text{ torr}$. 2.5 kW of radiofrequency (RF) waves at 2.45 GHz were injected into the vacuum vessel to ionize the gas molecules at the electron cyclotron resonance (ECR), which was held at a major radius (R) of $\approx 43\text{-}44 \text{ cm}$ to maximize B deposition on the inner wall PFCs. The ECDCs were carried out with helium-4 gas at $2.0 \times 10^{-4} \text{ torr}$. The first ECDC discharge was difficult to maintain with the ECR at $R \approx 43 \text{ cm}$ right on the PFC surface, resulting in only $\sim 50 \text{ min}$ of operation;

the second ECDC was maintained for the full 120 minutes with the ECR moved radially outwards to $R \approx 44$ cm. The 24 hour GDC was also conducted in helium-4 gas with an electrostatic potential of approximately 1000 V between the charged plates and the PFC surfaces; average in-vessel pressure was 2×10^{-2} torr.

It is important to understand the expected effects of each conditioning process on regions that AIMS can presently interrogate. The AIMS measurement locations are presently confined to ($\sim 35 \times 2$ cm vertical section) of the inner wall PFCs. Depositing B and using ECDC on the inner wall, however, is problematic as both B, which has been shown to exist as ions after breakup of the B_2D_6 molecule during BZN, are subject to a radially outward $\mathbf{E} \times \mathbf{B}$ drift that strongly inhibits ions from reaching the inner wall [13]. Thus, the B deposition rate rapidly falls to zero within a few centimeters radially inboard of the ECR, and ECDC has is likely to be minimally effective for cleaning those PFCs that are radially inboard of the ECR. In GDC, ions are accelerated to the walls electrostatically with no magnetic field present, and, therefore, we expect GDC to perturb the inner wall PFC surfaces.

4 AIMS measurements of deuterium retention during plasma operations

The results of AIMS measurements during wall conditioning appear in Figure 4, which shows the fractional changes in D and B relative to the first measurement, designated as $m = 0$; vertical labels on the figure indicate the plasma shots that occurred in between each AIMS measurement. The data is for a single PFC location approximately 8 cm below the midplane with the sequence of plasmas and AIMS measurements as shown in the timeline of Figure 2.

The most prominent feature is the nearly identical trends in the fractional change of D and B during both LSN and IWL plasma shots. The result corroborates the hypothesis that the plasma is eroding and redepositing D-saturated layers of B, which is of importance for understanding which physical retention mechanisms are responsible for fuel retention in low-Z

film-coated refractory metal PFCs. As discussed above, if some mechanism existed to deplete the B layer of D then there would be additional atomic capacity to store D via codeposition with B; however, the AIMS measurements show that the plasma is **eroding/redepositing B with a constant D/B ratio** since the fractional changes are identical and since there is no evidence of D depletion over the course of ≈ 35 s of plasma operation. Since the AIMS measurements took place well after a BZN, when the D/B ratio presumably stabilizes at the level of ~ 0.1 found during post-campaign analysis, **the AIMS result provides experimental evidence that the amount of available D capacity in the B layers is insufficient to explain the net D retention experimentally found in Alcator C-Mod.** This strongly suggests that D retention takes place via energetic ion implantation, diffusion, and retention in damaged or expanded trap sites in the bulk Mo PFCs.

Another prominent feature in the D and B trends is the distinct bifurcation from net deposition during the LSN shots to zero deposition (with a hint of net erosion) during the IWL shots. The first part of the trend is consistent with the expectations of material migration and redeposition in the boundary plasma from the outer divertor to the inner wall and divertor during LSN operation. Net deposition ceases immediately with the conclusion of the LSN shots, leading to either zero net deposition or more likely to net erosion of the B layer that is too small to be measured with the current sensitivity of AIMS.

Analysis of these AIMS measurements for absolute B erosion/deposition in this period have been published elsewhere [7]. In short, net deposition rates on the inner wall during LSN were measured at $\sim 5 \pm 3$ nm s⁻¹, consistent with previous estimates of 1-2 nm s⁻¹ [8]. Essentially zero net erosion was measured during the four IWL shots, consistent with very low levels of erosion expected in only ~ 8 s of plasma exposure.

At present, AIMS is limited to measuring only relative changes in D¹; however, the ability to measure absolute B layer thicknesses can provide a crude estimate of D codeposited with B. Analysis of these plasma-deposited B layers from Alcator C-Mod [14], TEXTOR [15], and

¹New neutron-based ion beam analysis techniques are now being developed for AIMS in an *ex-situ* laboratory that should lead to absolute D concentration measurements

laboratory experiments [16] have all found consistent D/B atomic ratios, typically saturated up to 0.4. Thus, the areal D deposition rate can be estimated as

$$R^D = R^B \cdot \frac{N^D}{N^B} \cdot \frac{\rho_m^B N_A}{A^B} \quad (1)$$

where R^B is the B deposition rate, $\frac{N^D}{N^B}$ is the D/B atomic ratio, ρ_m^B is the mass density of B (taken as 2.37 g cm^{-3} for elemental B), N_A is Avogadro's number, and A^B is the atomic weight of elemental B ($10.811 \text{ kg mol}^{-1}$). Using the AIMS measurement of $\sim 5 \text{ nm s}^{-1}$ and D/B ~ 0.4 gives a areal D deposition rate of $\sim 3 \times 10^{20} \text{ D m}^{-2} \text{ s}^{-1}$ on the inner wall PFCs.

As discussed in Section 2, D retention in B cannot be responsible for the continuous net D retention observed in Alcator C-Mod; however, accumulated layers of B can represent a significant inventory of D or, of more concern in a D-T device, T. Consider a typical D-T reactor-scale device ($R = 6 \text{ m}$, $a = 2 \text{ m}$, total PFC area $\sim 600 \text{ m}^2$) that might use BZN. If we assume an accumulated $5 \mu\text{m}$ B layer with a saturated atomic T/B ~ 0.4 , the result is $\sim 1 \times 10^{26}$ tritons, or about 0.8 kg T, stored in the B surface layer, which does not account for additional retention in the bulk PFCs. This simple exercise provides strong motivation to study fuel retention in micron-level films in present devices. Kilogram levels of in-vessel tritium is a serious nuclear hazard, potentially requiring suspension of device operation for cleaning, and probably makes sufficient tritium breeding in reactors infeasible.

5 AIMS measurements of deuterium retention during wall conditioning

The results of AIMS measurements during wall conditioning appear in Figure 5, which shows the fractional changes in D and B relative to the $m = 4$ measurement at four labeled locations on the inner wall PFCs (refer to the timeline of Figure 2 for chronology). Locations A, B, and C are located at a major radius of $R = 43 \text{ cm}$ while measurement location D is located at

$R = 46$ cm due to the “skirt” region of the lower inner wall that extends radially outwards approximately 3 cm from rest of the inner wall. The deuteron beam trajectories in the Alcator C-Mod vacuum vessel and PFC measurement locations are shown to the right of the figure for reference. Vertical labels on the graphics indicate the wall conditioning processes that occurred in between each AIMS measurement.

Of the three wall conditioning processing, BZN is the most well understood in terms of the induced physical changes to the PFC surfaces. For the upper three measurement locations (A, B, and C), the fractional increase in B as a result of BZN were 1.13 ± 0.09 , 1.09 ± 0.09 , and 1.16 ± 0.10 . The change in B at location D - ~ 3 cm radially outboard where the B deposition is known to be greater - was 1.65 ± 0.15 . The AIMS results have been shown to quantitatively agree with the radially dependent B deposition rates [6, 7] that were precisely measured with a quartz microbalance [13].

It is evident that the fractional changes of D and B are not tightly linked during wall conditioning as are during plasma operations. As discussed above, the intershot AIMS measurements corroborate the theory that the **plasma erodes, transports, and redeposits B layers with a constant D/B ratio**; however, as measured by AIMS, wall conditioning effects the B and D on the PFC surface differently. These condition processes, which occur throughout the plasma campaign, may, in addition to D outgassing after BZN, explain why saturated B layers with atomic ratios of ~ 0.4 are deposited during BZN, but post-campaign measurements measure only measure ~ 0.1 . It is clear that complex, anisotropic PMI is occurring during BZN, ECDC, and GDC, which results in the relative changes in D and B shown in Figure 5. Future AIMS experiments are now being planned to investigate these issues.

Finally, the results in Figure 5 demonstrate that the fractional increases of D are larger than those of B for locations A, B, and C ($R \approx 43$ cm); the reverse is true for location D ($R \approx 46$ cm), which shows a higher fractional increase in B compared to D. The result suggests that the majority of D, unlike the ionic deposition of B, deposits as neutral atoms

or molecules on the PFC surface after the diborane molecules are broken up during the BZN. Neutral D would not be subject to the $\mathbf{E} \times \mathbf{B}$ forces that effect the ionized B, resulting in D deposition being a far more isotropic process than B deposition. Thus, the fraction of D that deposits radially *inboard* of the ECR would be higher than for B, which is corroborated by the AIMS measurement of the PFCs at locations A, B, and C (0.5 cm inboard of the ECR). Conversely, roughly the same fraction of D deposits radially *outboard* of the ECR at location D, but, in this case, the fractional increase of B would be substantially higher due the peaked radial B deposition profiles. While the AIMS results are consistent with this explanation, further work is required to understand the spatial deposition of D in Alcator C-Mod during BZNs.

6 Summary

This paper has presented the first measurements of D fuel retention made with AIMS, a novel PMI technique that uses a 0.9 MeV beam of deuterons to remotely interrogate a large area of PFC surfaces *in-situ* with ~ 1 cm spatial resolution and shot-to-shot time resolution. *Relative measurements of the fractional change in D and B concentrations during LSN and IWL plasmas were presented, demonstrating that the plasma is eroding (during IWL) and redepositing (during LSN) B layers with a constant D/B ratio on inner wall PFCs.* The finding has important implications for understanding fuel retention in Alcator C-Mod. *Previous work has suggested that after a period of post-BZN D outgassing from B films the plasma erodes/redeposits B films with a constant D/B ratio of ~ 0.1 . The AIMS measurements - albeit on only a few shots - confirm this suggestion, finding no experimental evidence that the plasma somehow depletes and refills D to saturation in the B films, as needed to approach the level of net D retention observed in Alcator C-Mod. D retention in the bulk Mo PFCs, therefore, must be responsible.* Measurements of D and B concentrations on the inner wall during BZN, ECDC, and GDC were also presented, corroborating previous

conclusions for BZN that B deposits ionically with a deposition peak radially outboard of the ECR layer. The measurements also suggest that D deposits as neutrals isotropically on the first wall during BZN, potentially resulting in anisotropic D/B ratios across the first wall PFCs.

It should be noted that the data presented in this paper were acquired in only the first three hours of operating the proof-of-principle AIMS diagnostic on Alcator C-Mod. With its successful demonstration, major upgrades are being undertaken that will enable up to twenty intershot measurements, reduce measurement uncertainty, and improve magnetic steering access to a substantial portion of the total PFC area. Significant *ex-situ* laboratory work is also presently being performed to validate and enhance AIMS measurement capabilities, such as the ability to make absolute measurements of D concentration. Thus, for the first time in experimental PMI science, one can imagine routinely producing time-resolved maps of fuel retention, net erosion and deposition, and isotopic composition over a majority of PFC surfaces with AIMS on Alcator C-Mod.

The implementation of AIMS on a future superconducting, D-T burning tokamak to directly measure T retention is not as straightforward, as steady-state magnetic fields and a highly activated nuclear environment complicate beam steering and particle detection, respectively, although initial scoping studies to assess feasibility are encouraging. However, the application of AIMS in present nonsuperconducting D-D tokamaks will result in a tremendous advance in experimental PMI science - one could imagine constructing empirical, PFC-location dependent scaling laws for fuel retention, for example - and a wealth of high granularity experimental PFC surface data to guide the development and validation PMI modeling codes.

7 Acknowledgments

The authors are grateful to the outstanding engineering and technical staff at Alcator C-Mod and the MIT Plasma Science and Fusion Center. In particular, we would like to personally thank the following individuals who were crucial for the success of this diagnostic: Alan Binus, Gary Dekow, Bill Forbes, Jim Irby, Ron Rosati, David Terry, Tom Toland, and Rui Vieira. The authors would also like to thank George Engeman for his assistance with refurbishing the RFQ accelerator. This work is supported by U.S DOE Grant DE-FG02-94ER54235 and Cooperative Agreement DE-FC02-99ER54512.

References

- [1] M. A. Abdou, E. L. Vold, C. Y. Gung, M. Z. Youssef, K. Shin, Deuterium-tritium fuel self-sufficiency in fusion reactors, *Fusion Technology* 9 (1985) 250 – 285.
- [2] G. Federici, C. Skinner, J. Brooks, J. Coad, C. Grisolia, A. Haasz, A. Hassanein, V. Philipps, C. Pitcher, J. Roth, W. Wampler, D. Whyte, Plasma-material interactions in current tokamaks and their implications for next step fusion reactors, *Nuclear Fusion* 41 (12) (2001) 1967. doi:10.1088/0029-5515/41/12/218.
- [3] A. Semerok, C. Grisolia, {LIBS} for tokamak plasma facing components characterisation: Perspectives on in situ tritium cartography, *Nuclear Instruments and Methods in Physics Research Section A: Accelerators, Spectrometers, Detectors and Associated Equipment* 720 (0) (2013) 31 – 35, selected papers from the 2nd International Conference Frontiers in Diagnostic Technologies (ICFDT2). doi:<http://dx.doi.org/10.1016/j.nima.2012.12.042>.
URL <http://www.sciencedirect.com/science/article/pii/S0168900212015756>
- [4] Z. S. Hartwig, D. G. Whyte, Simulated plasma facing component measurements for an in situ surface diagnostic on Alcator C-Mod, *Review of Scientific Instruments* 81 (10) (2010) 10E106. doi:10.1063/1.3478634.
- [5] Z. S. Hartwig, H. S. Barnard, R. C. Lanza, B. N. Sorbom, P. W. Stahle, D. G. Whyte, An in situ accelerator-based diagnostic for plasma-material interactions science on magnetic fusion devices, *Review of Scientific Instruments* 84 (12) (2013) –. doi:<http://dx.doi.org/10.1063/1.4832420>.
- [6] Z. S. Hartwig, An in-situ accelerator-based diagnostic plasma-material interactions on magnetic fusion devices, Ph.D. thesis, Massachusetts Institute of Technology (2013).

- [7] H. S. Barnard, Development of Accelerator Based Spatially Resolved Ion Beam Analysis Techniques for the Study of Plasma Materials Interactions in Magnetic Fusion Devices, Ph.D. thesis, Massachusetts Institute of Technology (2014).
- [8] B. Lipschultz, D. Whyte, J. Irby, B. LaBombard, G. Wright, Hydrogenic retention with high-Z plasma facing surfaces in Alcator C-Mod, *Nuclear Fusion* 49 (4) (2009) 045009. URL <http://stacks.iop.org/0029-5515/49/i=4/a=045009>
- [9] W. Wampler, B. LaBombard, B. Lipschultz, G. McCracken, D. Pappas, C. Pitcher, Molybdenum erosion measurements in Alcator C-Mod, *Journal of Nuclear Materials* 266-269 (1999) 217 – 221. doi:10.1016/S0022-3115(98)00663-1.
- [10] Y. Lin, J. Irby, B. Lipschultz, E. Marmor, D. Whyte, S. Wolfe, S. Wukitch, Hydrogen control in Alcator C-Mod walls and plasmas, *Journal of Nuclear Materials* 363-365 (2007) 920 – 924, Plasma-Surface Interactions-17. doi:10.1016/j.jnucmat.2007.01.115.
- [11] R. A. Pitts, J. P. Coad, D. P. Coster, G. Federici, W. Fundamenski, J. Horacek, K. Krieger, A. Kukushkin, J. Likonen, G. F. Matthews, M. Rubel, J. D. Strachan, J.-E. contributors, Material erosion and migration in tokamaks, *Plasma Physics and Controlled Fusion* 47 (12B) (2005) B303. URL <http://stacks.iop.org/0741-3335/47/i=12B/a=S22>
- [12] D. Whyte, B. Lipschultz, J. Irby, R. Granetz, B. LaBombard, J. Terry, G. Wright, Hydrogenic fuel recovery and retention with metallic plasma-facing walls in the Alcator C-Mod tokamak, 2006, Proceedings of the 21st IAEA Conference on Fusion Energy. URL <http://www-naweb.iaea.org/napc/physics/fec/fec2006/html/node256.htm>
- [13] R. Ochoukov, D. G. Whyte, B. Lipschultz, B. LaBombard, N. Gierse, S. Harrison, Study and optimization of boronization in Alcator C-Mod using the Surface Science Station (S3), *Fusion Engineering and Design* 87 (9) (2012) 1700 – 1707. doi:10.1016/j.fusengdes.2012.07.013.

- [14] B. Lipschultz, Y. Lin, M. L. Reinke, A. Hubbard, I. H. Hutchinson, J. Irby, B. LaBombard, E. S. Marmor, K. Marr, J. L. Terry, S. M. Wolfe, the Alcator C-Mod group, D. Whyte, Operation of Alcator C-Mod with high-Z plasma facing components and implications, *Physics of Plasmas* 13 (5) (2006) 056117. doi:10.1063/1.2180767.
- [15] J. Winter, H. Esser, L. Knen, V. Philipps, H. Reimer, J. Seggern, J. Schlter, E. Vietzke, F. Waelbroeck, P. Wienhold, T. Banno, D. Ringer, S. Vepek, Boronization in TEXTOR, *Journal of Nuclear Materials* 162-164 (1989) 713 – 723. doi:10.1016/0022-3115(89)90352-8.
- [16] K. Tsuzuki, M. Natsir, N. Inoue, A. Sagara, N. Noda, O. Motojima, T. Mochizuki, T. Hino, T. Yamashina, Hydrogen absorption behavior into boron films by glow discharges in hydrogen and helium, *Journal of Nuclear Materials* 241-243 (1997) 1055 – 1059. doi:10.1016/S0022-3115(97)80193-6.

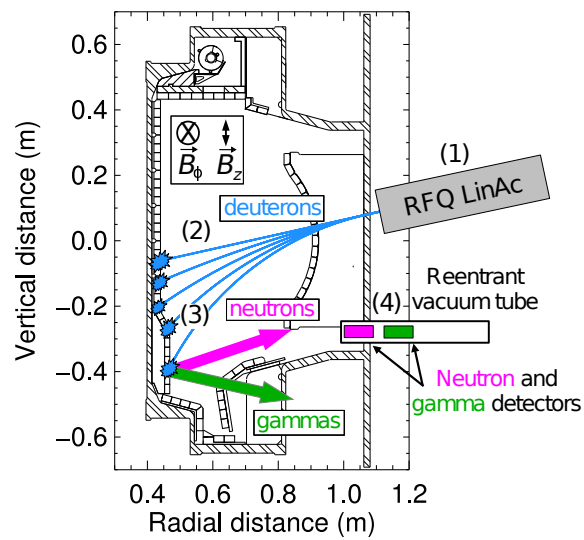


Figure 1: A depiction of the AIMS diagnostic on a poloidal cross section of the Alcator C-Mod tokamak showing (1) the RFQ linear accelerator, (2) the 0.9 MeV deuteron beam being magnetically steered within the vacuum vessel, (3) deuteron-induced nuclear reactions in the PFC surface, and (4) the reentrant neutron and gamma detectors. Magnetic steering provides a localized PFC surface measurement while the spectroscopy of induced neutrons and gammas enables the isotopic composition of the PFC surface to be reconstructed.

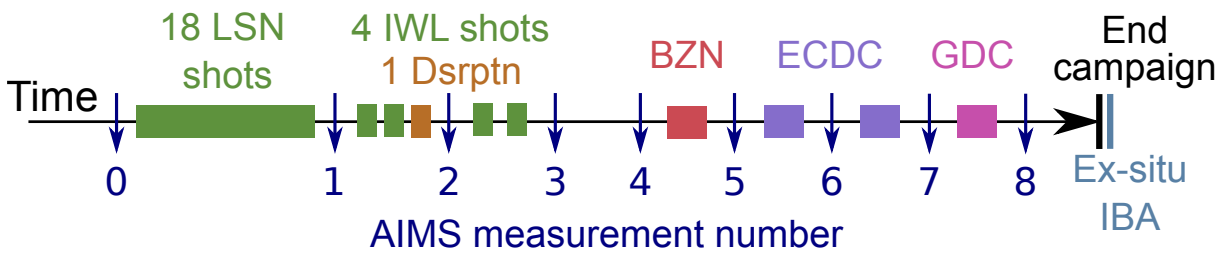


Figure 2: A timeline showing the sequence of plasma operations (above timeline) and AIMS PFC surface measurements (below timeline) carried out at the end of the FY12 plasma campaign; ex-situ ion beam analysis was performed immediately following the end the campaign.

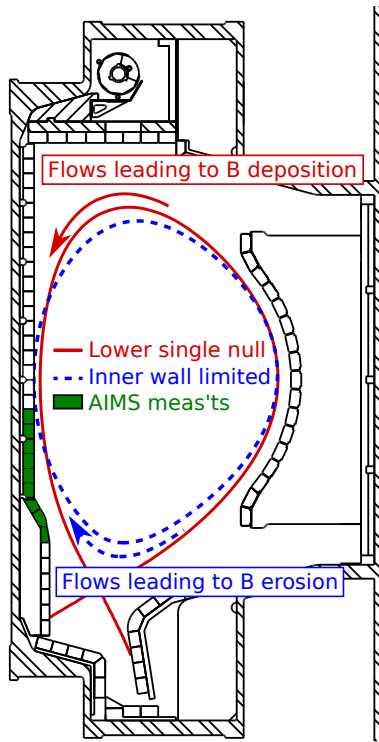


Figure 3: The last close flux surfaces for the lower single null (LSN) diverted shots (solid line) and the inner wall limited (IWL) shots (dashed line) with the PFCs accessible to AIMS (solid fill). The arrows indicate plasma flow that leads to net B deposition (erosion) at the AIMS measurement locations when the plasma is operated in LSN (IWL) configurations.

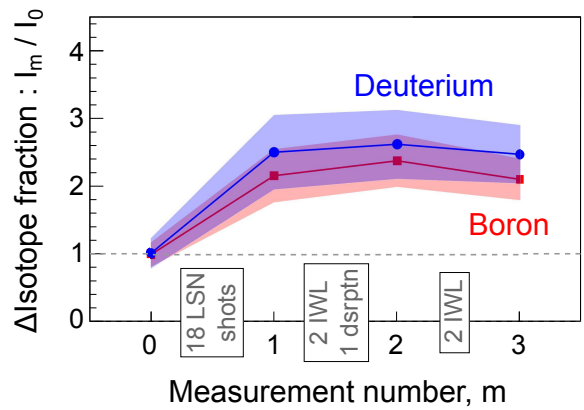


Figure 4: The measured fractional changes in D and B concentration relative to the first point ($m = 0$) on a single PFC on the inner wall just below the midplane. Plasma operations are noted in the boxes, and the measurement numbers correspond to those shown on the timeline in Figure 2.

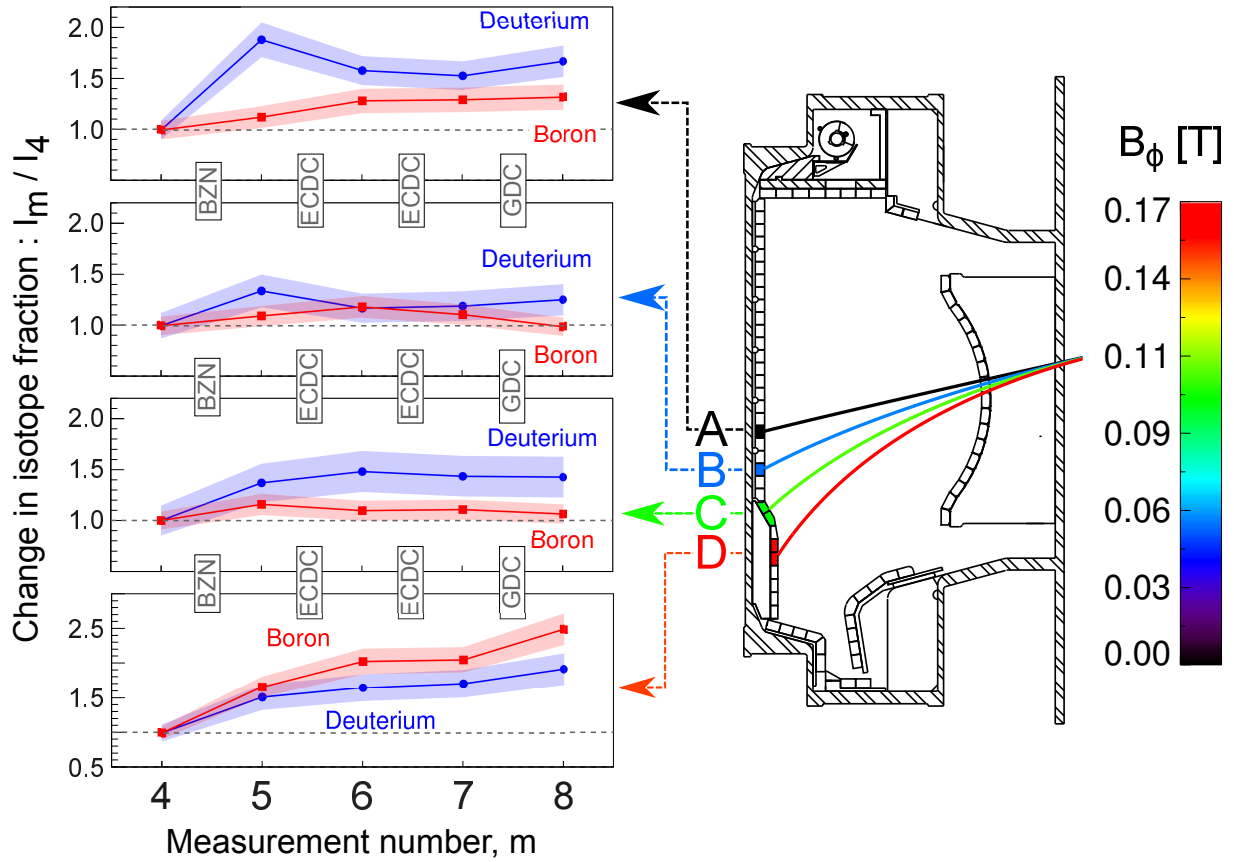


Figure 5: The measured fractional changes in D and B concentration relative to the first point ($m = 4$) at the four locations shown during wall conditioning experiments. The wall conditioning techniques are noted in the boxes, and the measurement numbers correspond to those shown on the timeline in Figure 2.